

# Black holes with a charged quantum dust core

R. Casadio<sup>ab\*</sup>, R. da Rocha<sup>c†</sup>, A. Giusti<sup>d‡</sup> and P. Meert<sup>e§</sup>

<sup>a</sup>*Dipartimento di Fisica e Astronomia, Università di Bologna  
via Iriero 46, 40126 Bologna, Italy*

<sup>b</sup>*I.N.F.N., Sezione di Bologna, I.S. FLAG  
viale B. Pichat 6/2, 40127 Bologna, Italy*

<sup>c</sup>*Federal University of ABC, Center of Mathematics  
Santo André, 09210-580, Brazil*

<sup>d</sup>*Department of Physics and Astronomy  
University of Sussex, Brighton, BN1 9QH, United Kingdom*

<sup>e</sup>*Instituto de Física Teórica, Unesp,  
São Paulo, 01140-070, Brazil*

November 14, 2024

## Abstract

To understand the nature of the black holes that exist in the Universe, it is also necessary to study what happens to the (quantum) matter that collapses and forms such objects. In this work, we consider a dust ball with an electrically charged central core and study its quantum spectrum by quantising the geodesic equation for individual dust particles in the corresponding Reissner-Nordström spacetime. As in the neutral case investigated previously, we find a ground state of the dust ball with the size of a fraction of the outer horizon. Moreover, we determine a self-consistent configuration of layers in the ground state corresponding to an effective mass function that increases linearly with the areal radius and has no inner Cauchy horizon. We then briefly speculate on the possible phenomenological consequences for the endpoint of the gravitational collapse.

---

\*E-mail: casadio@bo.infn.it

†E-mail: roldao.rocha@ufabc.edu.br

‡E-mail: A.Giusti@sussex.ac.uk

§E-mail: pedro.meert@unesp.br

# 1 Introduction

All of the known black hole solutions of General Relativity are characterised by the Arnowitt-Deser-Misner (ADM) [1] mass  $M$ , electric charge  $Q$ , and angular momentum  $J$ , and hide classical spacetime singularities inside the event horizon [2]. The existence of the horizon further implies that the spacetime is geodesically incomplete [3], which hints to possible violations of causality in the matter dynamics. The overall picture is particularly simple in the spherically symmetric Schwarzschild geometry, which essentially results from neglecting the matter that has collapsed to form it [4, 5], and the corresponding causal structure only contains the event horizon that hides the central singularity where certain geometric invariants built from the Riemann tensor diverge.

Non-trivial internal structures emerge as soon as one adds some matter source, like the electric field in the spherically symmetric Reissner-Nordström spacetime. In fact, beside the central singularity and outer event horizon, there now appears an inner Cauchy horizon, which was shown to cause potentially strong instabilities already long ago [6–9] (see also Refs. [10–16] for some more recent results). Since all of these issues are explicitly connected with the (inevitable) presence and behaviour of matter, one would hope that they can be resolved by properly taking into account the quantum nature of matter (and gravity), which has in fact been proposed in several approaches (see, *e.g.* Refs. [17–22]).

One of the few cases in which the gravitational collapse leading to black hole formation can be studied analytically is given by the Lemaître-Tolman-Bondi model [23–25] of a dust ball with ADM mass  $M$  and areal radius  $r = R_s(\tau)$ , where  $\tau$  is the proper time at the surface. Dust particles are not subjected to any pressure and follow geodesics in their own geometry [27], so that the density profile<sup>1</sup> shrinks during the collapse without changing shape. Many studies of this model start from a reduction of degrees of freedom based on spherical symmetry and continuity of the fluid used to describe the dust, which uniquely determine the interior Lemaître-Tolman-Bondi metric and the exterior Schwarzschild metric. From the Einstein-Hilbert action for such metrics (and the proper junction conditions at the surface), one can identify a few collective degrees of freedom, including the ball radius  $R_s$ , which can be canonically quantised (see, *e.g.* Refs. [28–35]).

The above approach to quantisation dispenses with the fact that astrophysical objects with enough mass to form a black hole must contain a huge number of matter particles.<sup>2</sup> Moreover, the classical Einstein field equations are analogous to thermodynamical laws [36] which, for black holes [37], appear to suggest an even larger number of gravitational excitations [38]. It seems therefore more appropriate to describe *a priori* a ball of dust with the quantum state for a very large number of particles of mass  $\mu$  and derive a collective description *a posteriori*. This is the alternative viewpoint advocated in Refs. [39, 40] for studying the case of dust without electric fields.

In order to preserve the (approximate) spherical symmetry, all particles are assumed to move radially without crossing paths and their number is large enough to form an “almost” continuous distribution. Moreover, since  $\mu \ll M$ , the back-reaction of individual particles on the local geometry is neglected by considering a course-grained layering of the ball, in which  $r = R_i(\tau)$  denotes trajectories on the inner border of the  $i^{\text{th}}$  layer [40]. Between the surfaces  $r = R_i(\tau)$  and  $r = R_{i+1}(\tau)$  should lie enough intermediate trajectories that the mass contribution of the particles at  $r = R_i(\tau)$  is negligible with respect to the total mass of the  $\nu_i \gg 1$  particles in the whole  $i^{\text{th}}$  layer defined by  $R_i \leq r < R_{i+1}$ . Birkhoff’s theorem then implies that particles following a trajectory with  $r = R_i$  are not affected by the particles at  $r = R_{j>i}$ , but only by those at  $r = R_{j<i}$ , whose number and

---

<sup>1</sup>In particular, the density is homogeneous in the Oppenheimer-Snyder [26] model.

<sup>2</sup> $M \simeq 10^{57} \mu$  for a solar mass object made of neutrons.

ADM mass do not change in time. Trajectories of dust particles (at the inner border of a given layer) are individually quantised and a condition is imposed to ensure that the fuzzy quantum layers defined by the positions of these particles remain orderly nested in the global quantum ground state in agreement with the uncertainty principle (see Ref. [40] and Section 2 for all the details).

Once the wavefunction  $\psi = \psi(r)$  for the ground state is obtained, an (effective) Misner-Sharp-Hernandez mass function [41, 42] for the core can be defined by

$$m(r) \equiv 4\pi \int_0^r \rho(x) x^2 dx \sim 4\pi \int_0^r |\psi(x)|^2 x^2 dx < \infty, \quad \text{for } r > 0, \quad (1.1)$$

where  $\rho = \rho(r)$  is the effective energy density [40]. In particular, one finds that  $m(r \rightarrow \infty) = M$  and

$$\rho \sim r^{-2} \quad \text{and} \quad m \sim r, \quad \text{for } r \rightarrow 0, \quad (1.2)$$

which ensures that  $m(0) = 0$  and the central curvature singularity of the vacuum Schwarzschild geometry [3] is replaced by an integrable singularity [43–45]. The centre of the core is, therefore, a region where the curvature invariants and the effective energy-momentum tensor diverge, but their volume integrals and tidal forces acting on radial geodesics remain finite [46].

It is well known that singularities which plague black hole solutions of the vacuum Einstein equations [3] can also be removed by imposing regularity conditions on the (effective) energy density and scalar invariants inspired by classical physics [47]. However, this procedure usually induces the existence of an inner Cauchy horizon, which is instead not the case for a mass function of the form in Eq. (1.2) [45]. As we recalled above, adding an electric field is the simplest way to induce the presence of a Cauchy horizon in the (otherwise empty) Reissner-Nordström spacetime. It is therefore interesting to further study the possible existence of inner horizons inside black holes by extending the previous investigations of the dust ball [39, 40] to include an electric charge  $Q$ .

The static and spherically symmetric line element

$$ds^2 = -f(r) dt^2 + \frac{dr^2}{f(r)} + r^2 d\Omega^2 \quad (1.3)$$

represents the vacuum Reissner-Nordström spacetime generated by a source of ADM mass  $M$  and charge  $Q$  for

$$f(r) = f_{\text{RN}} = 1 - \frac{2G_N M}{r} + \frac{G_N Q^2}{r^2}, \quad (1.4)$$

where  $G_N$  is Newton's constant. The metric function in Eq. (1.4) can have two (possibly degenerate) zeroes, associated with horizons, located at

$$R_{\pm} = G_N M \pm \sqrt{G_N^2 M^2 - G_N Q^2}, \quad (1.5)$$

provided

$$Q^2 \leq G_N M^2. \quad (1.6)$$

In particular, the sphere  $r = R_+$  is the outer event horizon and  $r = R_-$  is a Cauchy horizon [3].

In the present work, we shall consider the simplest case of a dust ball of ADM mass  $M$  with the charge  $Q$  localised inside a spherical innermost core of mass  $\mu_0 = \epsilon_0 M$  and radius  $r = R_1$ . This

core is surrounded by a number  $N \geq 1$  of electrically neutral layers of inner radius  $r = R_i$ , thickness  $\Delta R_i = R_{i+1} - R_i$ , and mass  $\mu_i = \epsilon_i M$ , where  $\epsilon_i$  is the fraction of ADM mass associated with the  $\nu_i$  dust particles in the  $i^{\text{th}}$  layer. The gravitational mass inside the ball  $r < R_i$  will be denoted by

$$M_i = \sum_{k=0}^{i-1} \mu_k = M \sum_{k=0}^{i-1} \epsilon_k, \quad (1.7)$$

with  $M_1 = \mu_0$  and  $M_{N+1} = M$ . The radius  $R_1$  and the mass  $M_1 = \mu_0$  of the innermost core, as well as the thickness  $\Delta R_i$  of each layer, can take arbitrarily small values in the classical picture, for example by increasing the number  $N$  of layers. In this configuration, dust particles on the inner surface of the  $i^{\text{th}}$  layer will move along radial geodesics (parameterized by the proper time  $\tau$ ),  $r = R_i(\tau)$ , of the Reissner-Nordström spacetime (1.3) with

$$f(r) = f_i = 1 - \frac{2G_N M_i}{r} + \frac{G_N Q^2}{r^2} \quad (1.8)$$

In particular, the mass-shell condition for the 4-velocity of components  $u_i^\mu = dx_i^\mu/d\tau = (\dot{t}_i, \dot{R}_i, 0, 0)$  yields the Hamiltonian constraint equation

$$H_i = \frac{P_i^2}{2\mu} - \frac{G_N \mu M_i}{R_i} + \frac{G_N \mu Q^2}{2R_i^2} = \frac{\mu}{2} \left( \frac{E_i^2}{\mu^2} - 1 \right) \equiv \varepsilon_i, \quad (1.9)$$

where  $P_i = \mu \dot{R}_i$  is the momentum conjugated to  $r = R_i(\tau)$ , and  $E_i$  is the conserved momentum conjugated to  $t_i = t_i(\tau)$ .<sup>3</sup> It is important to remark that we are assuming the mass  $\mu \ll M_i$  for all  $i = 0, \dots, N+1$  or, equivalently, the numbers  $\nu_i \gg 1$ , so that individual dust particles can be described as test particles with a good approximation.

Eq. (1.9) can be canonically quantised, similarly to the equation for the electron's trajectory in the quantum mechanical treatment of the hydrogen atom, and a spectrum of bound states will be found like in the neutral case [39, 40]. We will first analyse the bound states for dust particles at the surface of the ball following Ref. [39] in the next Section; a more refined description of the interior will then be obtained in Section 3 by considering multiple layers like in Ref. [40]; concluding remarks and outlook will be given in Section 4.

## 2 Dust ball with charged inner core

Dust particles on the surface of the ball of radius  $r = R_{N+1}(\tau) \equiv R_s$  will fall radially in the Reissner-Nordström metric defined by Eq. (1.8) with  $M_{N+1} = M$  and their geodesic motion will be described by the Hamiltonian constraint

$$H = \frac{P_s^2}{2\mu} - \frac{G_N \mu M}{R_s} + \frac{G_N \mu Q^2}{2R_s^2} = \frac{\mu}{2} \left( \frac{E^2}{\mu^2} - 1 \right) = \varepsilon, \quad (2.1)$$

where  $P_s = \mu \dot{R}_s$  is the momentum conjugated to  $R_s = R_s(\tau)$  and  $E$  is the conserved momentum conjugated to  $t = t_s(\tau)$ .

Canonical quantisation is obtained by replacing  $P_s \mapsto \hat{P}_s = -i\hbar \partial/\partial R_s$  and, after some manipulations, the time-independent Schrödinger-like equation

$$\hat{H} \Psi = \varepsilon \Psi \quad (2.2)$$

---

<sup>3</sup>The conserved angular momentum conjugated to  $\phi_i = \phi_i(\tau)$  vanishes for purely radial motion.

can be written as the generalised associated Laguerre equation <sup>4</sup>

$$\left( \frac{d^2}{dx^2} + \frac{2\mu^2 M}{\gamma \ell_p m_p^3 x} - \frac{\mu^2 Q^2}{\ell_p m_p^3 x^2} - \frac{1}{4} \right) \Psi = 0, \quad (2.3)$$

where  $x = \gamma R_s$  with

$$\gamma^2 = -\frac{8\mu\varepsilon}{m_p^2 \ell_p^2}. \quad (2.4)$$

Orthonormal solutions, in the scalar product

$$\langle \psi | \chi \rangle = 4\pi \int_0^\infty \psi^*(R_s) \chi(R_s) R_s^2 dR_s, \quad (2.5)$$

are then given by the wavefunctions

$$\Psi_{n\alpha}(R_s) = A_{n\alpha} e^{-\frac{\gamma}{2} R_s} r^{\frac{\alpha-1}{2}} L_{n-1}^\alpha(\gamma R_s), \quad (2.6)$$

where  $L_{n-1}^\alpha$  are generalised Laguerre polynomials of integer order  $n \geq 1$  and continuous parameter

$$\alpha^2 = 1 + \frac{4\mu^2 Q^2}{\ell_p m_p^3}, \quad (2.7)$$

from which one can see that  $|\alpha| \geq 1$ . The normalisation reads

$$A_{n\alpha}^2 = \frac{\gamma^{\alpha+2} \Gamma(n)}{4\pi^2 (2n + \alpha - 1) \Gamma^3(\alpha + n)}, \quad (2.8)$$

where  $\Gamma$  is the Euler gamma function. By introducing

$$\beta_{n\alpha} \equiv n + \frac{\alpha - 1}{2} = \frac{2\mu^2 M}{\gamma \ell_p m_p^3}, \quad (2.9)$$

the corresponding quantised energy spectrum  $\varepsilon = \varepsilon_{n\alpha}$  can be obtained by solving Eqs. (2.9) and (2.4) for  $\gamma$ , and reads

$$\varepsilon_{n\alpha} = -\frac{2\mu^3 M^2}{(2n + \alpha - 1)^2 m_p^4} = -\frac{\mu^3 M^2}{2\beta_{n\alpha}^2 m_p^4}, \quad (2.10)$$

which is discrete and bounded below. This implies the physically expected fact that an infinite amount of energy cannot be extracted from the system, in line with other quantum-mechanical descriptions of the Reissner-Nordström black holes, such as the Hamiltonian quantum theory of spherically symmetric and asymptotically flat electrovacuum spacetimes in Ref. [48].

The wavefunctions (2.6) can now be written as

$$\langle R_s | n\alpha \rangle = \Psi_{n\alpha}(R_s) = A_{n\alpha} \exp\left(-\frac{\mu^2 M R_s}{\beta_{n\alpha} \ell_p m_p^3}\right) R_s^{\frac{\alpha-1}{2}} L_{n-1}^\alpha\left(\frac{2\mu^2 M R_s}{\beta_{n\alpha} \ell_p m_p^3}\right), \quad (2.11)$$

where the integer  $n \geq 1$  and the value of  $\alpha$  is determined from the charge of the system according to Eq. (2.7). We also note that the quantised energy spectrum (2.10) is similar to the findings of Ref. [49], as it supports the existence of a lowest energy level. However, unlike the spectrum of the hydrogen atom, the quantised energy spectrum (2.10) depends not only on the charge  $Q$  and mass  $\mu$  of the dust particles but also on the total ADM mass  $M$  of the ball.

---

<sup>4</sup>We will often use units with  $G_N = \ell_p/m_p$  and  $\hbar = \ell_p m_p$ , where  $\ell_p$  is the Planck length and  $m_p$  the Planck mass.

## 2.1 Ball radius and uncertainty

The wavefunction (2.11) determines the probability distribution [in the scalar product (2.5)] for dust particles on the shell at the surface of the ball to be found at the radial position  $R_s$  given their mass  $\mu$  and the ball ADM mass  $M$ , with  $n$  and  $\alpha$  determined by  $M$  and the charge  $Q$  of the system. The overall size of the dust ball is therefore just given by the expectation value

$$\langle n\alpha | \hat{R}_s | n\alpha \rangle = \frac{12 \beta_{n\alpha}^2 - \alpha^2 + 1}{4 \beta_{n\alpha} \gamma_{n\alpha}}, \quad (2.12)$$

where we used  $\hat{R}_s | n\alpha \rangle = R_s | n\alpha \rangle$  and defined

$$\gamma_{n\alpha}^2 = -\frac{8 \mu \varepsilon_{n\alpha}}{m_p^2 \ell_p^2} = \frac{4 \mu^4 M^2}{\beta_{n\alpha}^2 \ell_p^2 m_p^6}. \quad (2.13)$$

Taking  $\gamma_{n\alpha} > 0$  yields

$$\langle n\alpha | \hat{R}_s | n\alpha \rangle = \frac{\ell_p m_p^3}{8 \mu^2 M} (12 \beta_{n\alpha}^2 - \alpha^2 + 1). \quad (2.14)$$

It is also important to estimate the quantum uncertainty for the size of the ball. From

$$\langle n\alpha | \hat{R}_s^2 | n\alpha \rangle = \frac{20 \beta_{n\alpha}^2 - 3 \alpha^2 + 7}{2 \gamma_{n\alpha}^2}, \quad (2.15)$$

and the definition of the variance  $\Delta R_s \equiv \sqrt{\langle \hat{R}_s^2 \rangle - \langle \hat{R}_s \rangle^2}$ , we obtain the ratio

$$\frac{\Delta R_s}{\langle n\alpha | \hat{R}_s | n\alpha \rangle} = \frac{\sqrt{\langle n\alpha | \hat{R}_s^2 | n\alpha \rangle - \langle n\alpha | \hat{R}_s | n\alpha \rangle^2}}{\langle n\alpha | \hat{R}_s | n\alpha \rangle} = \frac{\sqrt{16 \beta_{n\alpha}^2 (\beta_{n\alpha}^2 + 2) - (\alpha^2 - 1)^2}}{12 \beta_{n\alpha}^2 - \alpha^2 + 1}. \quad (2.16)$$

which is a measure of how fuzzy the dust ball is in the state  $|n\alpha\rangle$ . The relevance of this result will become clearer in the following.

## 2.2 Ground state

In General Relativity, the conserved momentum  $E^2 \geq 0$ , which carries on to the quantum theory by constraining (from below) the possible values of the quantum number  $n$  [39, 40]. In particular, the ground state is defined by the minimum value  $E^2 = 0$ , which is equivalent to  $\varepsilon = -\mu/2$  from the right-most equality in Eq. (2.1). The corresponding value of  $\gamma$  can be determined from Eq. (2.4), namely

$$\gamma_{n\alpha} = \frac{2 \mu}{m_p \ell_p} \equiv \gamma_\mu, \quad (2.17)$$

and leads to the minimum value of

$$\beta_{n\alpha} = \frac{\mu M}{m_p^2} \equiv \beta_M. \quad (2.18)$$

The integer quantum number  $n$  corresponding to the ground state can finally be expressed in terms of the ADM mass  $M$ , dust particle mass  $\mu$ , and charge  $Q$  by substituting Eqs. (2.18) and (2.7) into Eq. (2.9), to wit

$$n = \frac{\mu M}{m_{\text{p}}^2} + \frac{1}{2} \left( 1 - \sqrt{1 + \frac{4Q^2 \mu^2}{m_{\text{p}}^3 \ell_{\text{p}}}} \right) \equiv N_{MQ} . \quad (2.19)$$

Since  $n \geq 1$ , the above implies the condition

$$\frac{\mu M}{m_{\text{p}}^2} - \frac{1}{2} \sqrt{1 + \frac{4Q^2 \mu^2}{m_{\text{p}}^3 \ell_{\text{p}}}} \geq \frac{1}{2} , \quad (2.20)$$

that is, the ADM mass and charge must satisfy <sup>5</sup>

$$G_{\text{N}} M^2 \geq Q^2 + M (\hbar/\mu) > Q^2 , \quad (2.21)$$

which is therefore stronger than the classical condition (1.6) for the existence of (two) horizons. In particular, Eq. (2.21) excludes the exact classical extremal case  $R_- = R_+$  obtained for  $G_{\text{N}} M^2 = Q^2$  (see Appendix A for more details).

The expectation value of the size of the ball in the ground state is obtained by direct substitution of Eqs. (2.18) and (2.17) into Eq. (2.12), and yields

$$\langle \hat{R}_{\text{s}} \rangle \equiv \langle N_{MQ} | \hat{R}_{\text{s}} | N_{MQ} \rangle = \frac{3}{2} G_{\text{N}} M \left( 1 - \frac{Q^2}{3 G_{\text{N}} M^2} \right) , \quad (2.22)$$

so that the core has a finite radius of size

$$G_{\text{N}} M < \langle \hat{R}_{\text{s}} \rangle \leq \frac{3}{2} G_{\text{N}} M . \quad (2.23)$$

On comparing Eqs. (2.22) and (1.5) we see that the ball in the ground state lies inside the classical outer horizon if  $\langle \hat{R}_{\text{s}} \rangle < R_+$ . Given the condition in Eq. (2.21), this implies

$$\sqrt{1 - \frac{Q^2}{G_{\text{N}} M^2}} < 2 , \quad (2.24)$$

which is always satisfied and we can say that all consistent ground states represent black holes. It is then interesting to investigate if the ground state can lie inside the classical inner horizon,  $\langle \hat{R}_{\text{s}} \rangle < R_-$ . This would happen for

$$\sqrt{1 - \frac{Q^2}{G_{\text{N}} M^2}} < -2 , \quad (2.25)$$

which cannot be met, again because of the condition given by Eq. (2.21). The overall conclusion is that all consistent quantum ground states are black holes without a Cauchy inner horizon (see Fig. 1 and further comments below <sup>6</sup>).

<sup>5</sup>For  $Q = 0$ , this condition implies that the Schwarzschild radius must be sufficiently larger than the Compton length of one dust particle,  $R_{\text{H}} = 2 G_{\text{N}} M > 2 \hbar/\mu$  (see also Refs. [50–52]).

<sup>6</sup>In numerical plots we employ dimensionless quantities given by  $\tilde{M} = M/m_{\text{p}}$ ,  $\tilde{\mu} = \mu/m_{\text{p}}$ ,  $\tilde{Q}^2 = Q^2/\ell_{\text{p}} m_{\text{p}}$ ,  $\langle \tilde{R}_{\text{s}} \rangle = \langle \hat{R}_{\text{s}} \rangle/\ell_{\text{p}}$ .

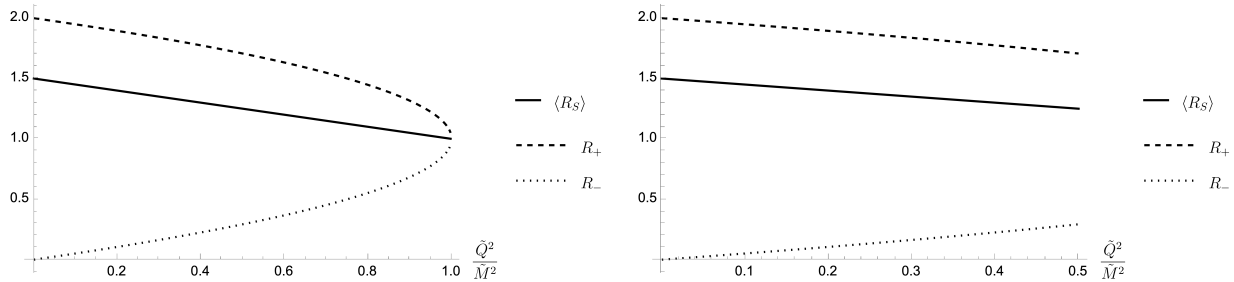


Figure 1: Ball radius  $\langle \hat{R}_s \rangle$  and horizon radii  $R_{\pm}$  for  $\tilde{M} = 10^3$  with  $\tilde{\mu} = 1$  (left panel) and  $\tilde{\mu} = 2 \cdot 10^{-3}$  (right panel):  $R_- < \langle \hat{R}_s \rangle < R_+$  for all allowed values of the charge  $Q$  that satisfy the condition (2.21) depending on  $\tilde{\mu}$ . (Tilded quantities are dimensionless variables defined in Footnote 6.)

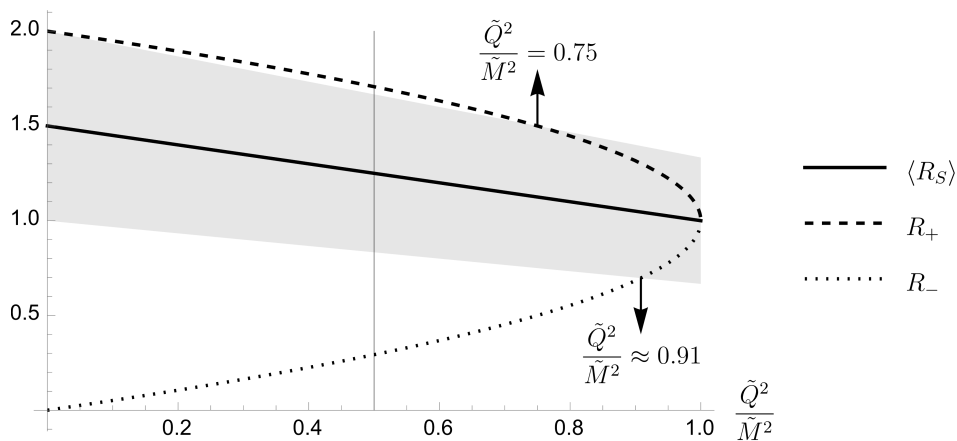


Figure 2: Ball radius  $\langle \hat{R}_s \rangle$  and horizon radii  $R_{\pm}$  as functions of the charge-to-mass ratio. Note that  $R_- < \langle \hat{R}_s \rangle < R_+$  for all classically allowed values of the charge  $\tilde{Q}^2 \leq \tilde{M}^2$ . Shaded band represents the fuzzy region bounded by  $\langle \hat{R}_s \rangle \pm \Delta R_s$ . Arrows indicate values where the (event or Cauchy) horizon radius enters the fuzzy region. Thin vertical line indicates the maximum value of the charge-to-mass ratio from the right panel of Fig. 1. (Tilded quantities are dimensionless variables defined in Footnote 6.)

We conclude this part by looking at the uncertainty (2.16) for the size of the the ground state with  $n = N_{MQ}$  for astrophysical objects with

$$\beta_M = \mu M/m_p^2 \gg 1. \quad (2.26)$$

In this case, we expect that the charge is much smaller than the mass, that is  $Q^2 \ll G_N M^2$ , so that  $\alpha \sim 1$  and  $N_{MQ} \gg 1$ . We can expand Eq. (2.16) in this regime to obtain

$$\frac{\Delta R_s}{\langle \hat{R}_s \rangle} \simeq \frac{1}{3} + \frac{11 + \alpha^2}{36 \beta_M^2} \simeq \frac{1}{3} \left[ 1 + \frac{m_p^4}{\mu^2 M^2} \left( 1 + \frac{2\mu^2 Q^2}{3 \ell_p m_p^3} \right) \right] \simeq \frac{1}{3}, \quad (2.27)$$

where the last approximation comes from our assumption in Eq. (2.26). In particular, we notice that the size  $R_s$  of the quantum ball is fuzzy and should approximately lie within the interval



$|R_s - \langle \hat{R}_s \rangle| \leq \Delta R_s$ , where

$$\langle \hat{R}_s \rangle - \Delta R_s \simeq \frac{2}{3} \langle \hat{R}_s \rangle \simeq G_N M - \frac{Q^2}{3M} \quad (2.28)$$

and

$$\langle \hat{R}_s \rangle + \Delta R_s \simeq \frac{4}{3} \langle \hat{R}_s \rangle \simeq 2 G_N M - \frac{2Q^2}{3M} . \quad (2.29)$$

This range is represented by the shaded region in Fig. 2 (for the same values of  $M$  and  $\mu$  used in the left panel of Fig. 1 so that the maximum value of  $Q^2 \simeq G_N M^2$ ).

We notice in particular that the upper boundary (2.29) is shorter than the classical event horizon at  $r = R_+$  if

$$1 - \frac{2Q^2}{3G_N M^2} < \sqrt{1 - \frac{Q^2}{G_N M^2}} , \quad (2.30)$$

equivalent to  $4Q^2 < 3G_N M^2$ . The matter core could therefore be found with a larger radius than the outer horizon  $R_+$  for  $Q^2/G_N M^2 \gtrsim 0.75$  (see the upward arrow in Fig. 2). This also implies that a dust ball of charge close to the extremal classical case  $Q^2 = G_N M^2$  would very likely not be a classical black hole at all,<sup>7</sup> meaning that the probability of finding dust particles placed at  $r > R_+$  is not negligible (see, *e.g.* Refs. [50, 51, 54]). Likewise, the lower boundary (2.28) is shorter than the inner horizon  $R_-$  if

$$\sqrt{1 - \frac{Q^2}{G_N M^2}} < \frac{Q^2}{3G_N M^2} , \quad (2.31)$$

which means that dust particles at the surface of the matter core could be found inside the classical Cauchy horizon  $R_-$  with significant probability provided  $Q^2/G_N M^2 \gtrsim 0.91$  (see the downward arrow in Fig. 2). The relevance of these results is that they further clarify the proper quantum nature of the matter core and ensuing geometry.

### 3 Multilayer core

We now want to improve on the previous description of the dust ball by considering several layers surrounding the innermost core where the charge is located, as described in the Introduction. The solution for Eq. (1.9) is of the same form as Eq. (2.6), namely

$$\langle R_i | n_i \alpha \rangle \equiv \Psi_{n_i \alpha}(R_i) = A_{n_i \alpha} e^{-\frac{\gamma_i}{2} R_i} R_i^{\frac{\alpha-1}{2}} L_{n_i-1}^\alpha(\gamma_i R_i) . \quad (3.1)$$

where  $r = R_i$  is the areal radius of dust particles located on the surface that identifies the inner border of the  $i^{\text{th}}$  layer and the integer  $n_i \geq 1$  labels their quantum state. Similarly to what was done in Section 2, we define the parameters

$$\beta_{n_i \alpha} \equiv n_i + \frac{\alpha - 1}{2} = \frac{2\mu^2 M_i}{\gamma_i \ell_p m_p^3} , \quad (3.2)$$

---

<sup>7</sup>Similar results were previously obtained in Refs. [44, 53].

where now  $\gamma_i$  is associated with the energy levels of each shell  $\varepsilon_i$  by

$$\gamma_i^2 = -\frac{8\mu\varepsilon_i}{m_p^2\ell_p^2}, \quad (3.3)$$

and  $\alpha$  is still given by Eq. (2.7) for all of the layers.

Substituting everything back in Eq. (3.1) we obtain the spectrum

$$\Psi_{n_i\alpha}(R_i) = A_{n_i\alpha} \exp\left(-\frac{\mu^2 M_i R_i}{\beta_{n_i\alpha} m_p^3 \ell_p}\right) R_i^{\frac{\alpha-1}{2}} L_{n_i-1}^\alpha\left(\frac{2\mu^2 M_i R_i}{\beta_{n_i\alpha} m_p^3 \ell_p}\right), \quad (3.4)$$

where

$$A_{n_i\alpha}^2 = \frac{\Gamma(n_i)}{8\beta_{n_i\alpha}\pi^2\Gamma^3(\alpha+n_i)} \left(\frac{2\mu^2 M_i}{\beta_{n_i\alpha} m_p^3 \ell_p}\right)^{\alpha+2}, \quad (3.5)$$

with eigenvalues

$$\varepsilon_{n_i\alpha} = -\frac{\mu^3 M_i^2}{2\beta_{n_i\alpha}^2 m_p^4}. \quad (3.6)$$

These results are a simple generalisation of the approach to the global radius of the ball employed in Section 2, and will be used it to describe a compact core for the black hole formed by layers identified by particles located on their inner borders.

### 3.1 Single ground states

Following the procedure used in Section 2.2, particles in the ground state of each layer will have energy  $\varepsilon_i = -\mu/2$ , equivalent to  $E_i^2 = 0$ , from Eq. (2.1). Correspondingly, we obtain  $\gamma_i = \gamma_\mu$  in Eq. (2.17) and

$$\beta_{n_i\alpha} = \frac{\mu M_i}{m_p^2} \equiv \beta_i. \quad (3.7)$$

The quantum number for dust particles in the ground state of each layer is therefore given by Eq. (2.19) with  $M = M_i$  and reads

$$n_i = \frac{\mu M_i}{m_p^2} + \frac{1}{2} \left(1 - \sqrt{1 + \frac{4Q^2\mu^2}{m_p^3\ell_p}}\right) \equiv N_i. \quad (3.8)$$

From this result, we use Eq. (2.12) to obtain the expectation value of each shell,

$$\langle \hat{R}_i \rangle \simeq \frac{3}{2} G_N M_i \left(1 - \frac{Q^2}{3G_N M_i}\right), \quad (3.9)$$

and, from the leading term in Eq. (2.27) for  $\beta_i \gg 1$ , the uncertainty

$$\Delta R_i = \sqrt{\langle \hat{R}_i^2 \rangle - \langle \hat{R}_i \rangle^2} \simeq \frac{1}{3} \langle \hat{R}_i \rangle. \quad (3.10)$$

These ground states are well defined provided the charge and discrete mass function  $M_i$  satisfy the condition given by Eq. (2.21), that is

$$G_N M_i^2 \geq Q^2 + M_i (\hbar/\mu) > Q^2. \quad (3.11)$$

Since  $M_i > M_{i-1}$ , the strongest constraint comes from  $i = 1$ , that is

$$Q^2 < G_N \mu_0^2, \quad (3.12)$$

where we used  $M_1 = \mu_0$  for the ADM mass of the central core.

### 3.2 Global ground state

Having generalised the construction for the global radius and the ground state expressions to individual layers, we can now study a matter core of dust for the charged black holes made of nested layers around a central charged core. In particular, the number  $N$  of layers and the (discrete) mass function  $m(R_i) = M_i$  for the ground state is still to be determined. Like in Ref. [40], we can find a self-consistent ground state by requiring that each layer of radius  $\langle \hat{R}_i \rangle$  in Eq. (3.9) have a thickness given by the uncertainty  $\Delta R_i$  in Eq. (3.10).

The above assumption implies that

$$\langle \hat{R}_{i+1} \rangle \simeq \langle \hat{R}_i \rangle + \Delta R_i \simeq \frac{4}{3} \langle \hat{R}_i \rangle, \quad (3.13)$$

which reproduces Eq. (2.22) for the surface of the ball with  $i = N$ . This straightforwardly leads to the condition

$$3 M_{i+1} - \frac{Q^2}{G_N M_{i+1}} \simeq 4 M_i - \frac{4 Q^2}{3 G_N M_i}, \quad (3.14)$$

which indeed reduces to the expected relation for the neutral case  $3 M_{i+1} = 4 M_i$  for  $Q = 0$  [40].

We will solve Eq. (3.14) for the discrete mass function numerically. It is again convenient to use the dimensionless quantities defined in Footnote 6, so that the equation now reads

$$3 \tilde{M}_{i+1} - \frac{\tilde{Q}^2}{\tilde{M}_{i+1}} - 4 \tilde{M}_i + \frac{4 \tilde{Q}^2}{3 \tilde{M}_i} = 0. \quad (3.15)$$

The constraints (3.11) also read

$$\tilde{M}_i^2 - \frac{\tilde{M}}{\tilde{\mu}} - \tilde{Q}^2 > 0. \quad (3.16)$$

We can solve Eqs. (3.15) recursively by starting from the total ADM mass  $M = M_{N+1}$ . The mass  $M_N$  inside the outermost layer is then given by the positive solution of Eq. (3.15) with  $i = N$ , and the process is repeated by solving Eq. (3.15) with  $M_{N+1} \mapsto M_N$ , and so on for  $i \mapsto i - 1$ . In this way, the mass inside the  $i^{\text{th}}$  layer can be obtained as long as Eq. (3.16) is satisfied, say up to  $i = N - k$ , for which we stop and assume  $M_{N-k} = M_0$  is the central core containing the charge  $Q$ . The number of layers  $N = k$  for a given ADM mass and charge is thus determined consistently.

A few results of the above procedure are displayed in Figs. 3 and 4, for different values of  $\tilde{M}$ ,  $\tilde{\mu}$  and  $\tilde{Q}$  chosen so that  $M \gg \mu$  and the plots are easier to read. By comparing the different plots, one can see that heavier dust particles lead to the formation of more layers, and most of these layers are closer to the central core [in agreement with the uncertainty (3.10)]. As expected, the number of layers decreases for larger charge  $\tilde{Q}$ , since the inequality (3.16) saturates for smaller values of  $k$ . It is particularly interesting to notice that the (dimensionless) discrete mass function is essentially linear in the (dimensionless) layer radius

$$\langle \tilde{R}_i \rangle = \frac{3}{2} \tilde{M}_i \left( 1 - \frac{\tilde{Q}^2}{3 \tilde{M}_i^2} \right). \quad (3.17)$$

This feature also appears in the neutral case [40].

The right panels in Figs. 3 and 4 show the discrete mass function  $M = M(R_i)$ , and we can clearly see a linear behaviour, except near the extremal case  $\tilde{Q} \simeq \tilde{M}$ . In that limiting regime, our analysis implies that the core would only admit one layer (on top of the central charged core), which is also in qualitative agreement with the fuzziness of the ball radius discussed in Section 2.2.

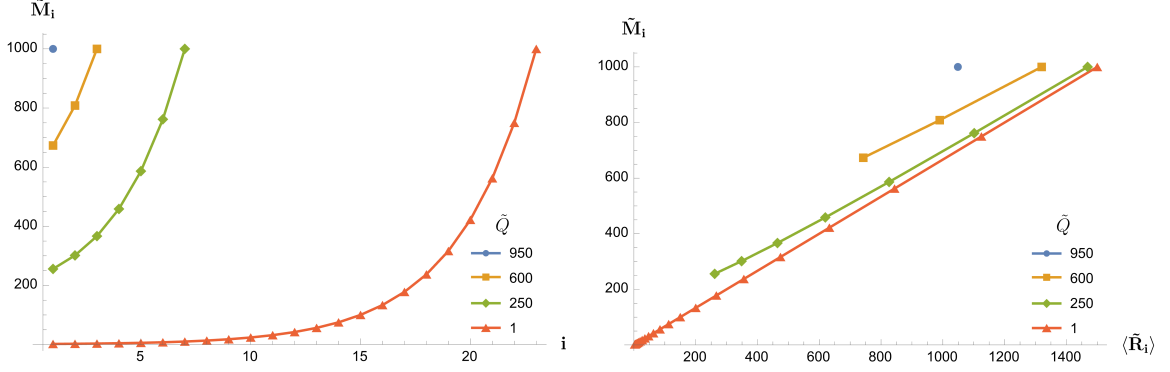


Figure 3: Discrete mass function  $m = M_i$  as function of the layer  $i$  (left panel) and areal radius  $\langle \tilde{R}_i \rangle$  (right panel) for  $\tilde{M} = 10^3$ ,  $\tilde{\mu} = 1$  and different values of  $\tilde{Q}$ .

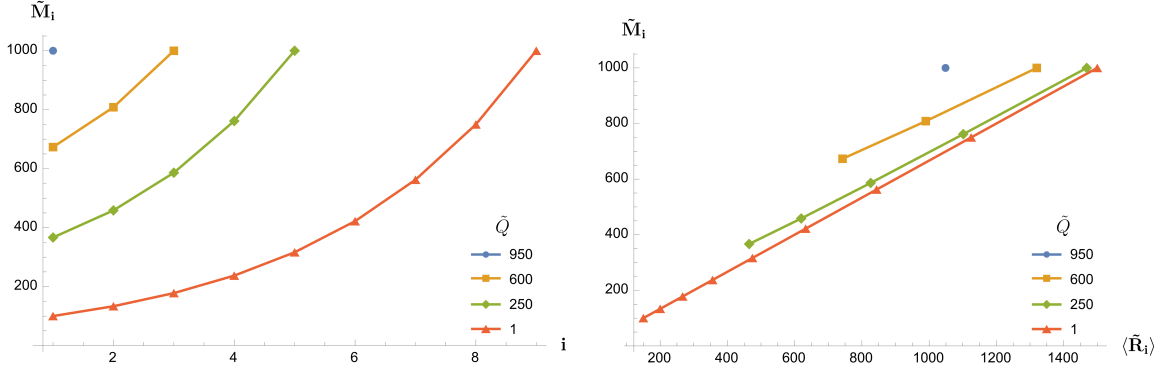


Figure 4: Discrete mass function  $m = M_i$  as function of the layer  $i$  (left panel) and areal radius  $\langle \tilde{R}_i \rangle$  (right panel) for  $\tilde{M} = 10^3$ ,  $\tilde{\mu} = 10^{-2}$  and different values of  $\tilde{Q}$ .

### 3.3 Effective metric and energy-momentum tensor

The discrete mass function  $M = M(R_i)$  obtained numerically in the previous section can be approximated by the continuous function

$$m \simeq K r , \quad (3.18)$$

where  $K \simeq 2/3 G_N$  for  $Q^2 \ll G_N M^2$  (see Figs. 3 and 4). This mass function corresponds to an effective quantum metric inside the dust ball given by Eq. (1.3) with <sup>8</sup>

$$f = f_q \simeq -1 + 2 G_N K - \frac{G_N Q^2}{r^2} . \quad (3.19)$$

The positive zeros of  $f_q$  would locate the possible horizons inside the dust ball, namely

$$r_-^2 \simeq \frac{G_N Q^2}{3} . \quad (3.20)$$

<sup>8</sup>The metric signature is  $+ - + +$  ( $r$  is a time coordinate) for  $r < \langle \hat{R}_s \rangle < R_+$ .

However, the charge  $Q$  must satisfy the condition (3.12), which implies that  $r_-^2 < G_N^2 \mu_0^2/3$  and lies inside the central core of mass  $M_1 = \mu_0$ , where the effective metric (3.19) cannot be employed. We also remark that the geometry in the region outside the ball will be given by the vacuum Reissner-Nordström metric (1.4) for  $r > \langle \hat{R}_s \rangle$  and one still has the outer event horizon  $R_+$ .<sup>9</sup> These results are in agreement with the analysis in Sections 2.1 and 3.2.

From the above metric, we can then compute the Einstein tensor  $G^\mu{}_\nu = 8\pi G_N T^\mu{}_\nu$  and determine the effective energy density and pressure

$$\rho = -T^r{}_r \simeq \frac{K}{4\pi r^2} + \frac{Q^2}{8\pi r^4} = -T^t{}_t \simeq -p_r, \quad (3.21)$$

and the effective tension

$$p_\perp = T^\theta{}_\theta \simeq \frac{Q^2}{8\pi r^4}. \quad (3.22)$$

These effective quantities reproduce the expressions in Ref. [40] for the neutral case  $Q = 0$  with the same value of  $K \simeq 2/3 G_N$ .<sup>10</sup>

It is important to notice that the term proportional to  $Q^2$  in the energy density Eq. (3.21) is not integrable but would correspond to the electric field contribution to the standard Reissner-Nordström singularity if the charge were localised at  $r = 0$ . As we discussed in the Introduction, we instead assume that the charge is distributed over the innermost core of finite radius  $\langle \hat{R}_1 \rangle \simeq G_N M_1 > 0$  given by Eq. (3.9) with  $i = 1$ . Eqs. (3.21) and (3.22) therefore only hold for  $\langle \hat{R}_1 \rangle < r < \langle \hat{R}_s \rangle$  (see Figs. 3 and 4 for examples of values taken by  $\langle \hat{R}_1 \rangle$ ).

## 4 Concluding remarks

We investigated a dust ball of mass  $M$  with electric charge  $Q$  localised inside a central massive core surrounded by electrically neutral layers of dust particles governed by the general relativistic dynamics. All dust particles would classically fall along radial geodesics in a Reissner-Nordström metric with suitable mass function, which results in the Hamiltonian constraint Eq. (1.9).

This constraint equation is canonically quantised similarly to the one describing the motion of the electron in the hydrogen atom and yields the discrete spectrum Eq. (3.4) for the dust particles in terms of generalised associated Laguerre polynomials with indices determined by the mass (function) and electric charge. The thickness of each layer is also related to the quantum uncertainty in the (radial) localisation of particles therein.

The system was solved explicitly for the ground state, which can exist only if the charge and mass function satisfy the bound in Eq. (3.11). In particular, these conditions ensure that the dust ball in the ground state is a black hole, since all of the dust is localised inside the outer horizon of the Reissner-Nordström metric, but tidal forces remain finite everywhere, so that there is no physically dangerous singularity in the centre. Moreover, the classically extremal case cannot be realised and the presence of an inner Cauchy horizon is further excluded. These two results are particularly noteworthy and stem from the finite spatial size of the ground state.

The main difference with respect to the neutral case studied in Refs. [39,40] is that the quantum numbers for the layers in the ground state are always very large for a ball of astrophysical mass if

<sup>9</sup>The precise matching of  $f_q$  with  $f_{RN}$  at  $r = \langle \hat{R}_s \rangle$  requires a better approximation for both effective metrics which is left for future developments.

<sup>10</sup>From Figs. 3 and 4, we see that  $K$  decreases slightly for larger  $Q$ .

$Q = 0$  but can be of order one if the charge approaches the limiting value allowed by the bound Eq. (2.21). Beside this technical aspect, the addition of an electric charge  $Q$  at the centre does not alter the main features previously found in the completely neutral model, which further supports the physical solidity of our approach to quantisation.

If the ground states obtained in Ref. [40] and in Section 3.2 were indeed to describe the endpoint of the gravitational collapse, one could conclude that no physically dangerous singularity is formed and the absence of a Cauchy horizon further removes known potential sources of instability for those configurations. The existence of a very large (quantum) matter core inside the horizon can then have potentially very interesting consequences for physical processes occurring in the outer region that can therefore be detected, as shown, *e.g.* in Ref. [55]. The detailed analysis of such effects is left for future publications.

## Acknowledgments

R.C. is partially supported by the INFN grant FLAG. R.dR. is grateful to the São Paulo Research Foundation FAPESP (grants No. 2024/05676-7 and No. 2021/01089-1) and CNPq (grants No. 303742/2023-2 and No. 401567/2023-0) for partial financial support. A.G. is supported in part by the Science and Technology Facilities Council (grants No. ST/T006048/1 and ST/Y004418/1). P.M. thanks FAPESP for the financial support (grants No. 2022/12401-9 and No. 2023/12826-2). The work of R.C. and A.G. has also been carried out in the framework of activities of the National Group of Mathematical Physics (GNFM, INdAM).

## A Charge constraints for the ground state and extremal case

The expectation value  $\langle \hat{R}_s \rangle$  of the ball radius in Eq. (2.22) is positive provided

$$12\beta_M^2 - \alpha^2 + 1 > 0. \quad (\text{A.1})$$

From Eq. (2.16) with  $\beta_{n\alpha} = \beta_M = \mu M/m_p^2$ , its uncertainty  $\Delta R_s$  is also positive if

$$16\beta_M^2 (\beta_M^2 + 2) - (\alpha^2 - 1)^2 > 0. \quad (\text{A.2})$$

Using the definition in Eq. (2.7), these inequalities read

$$\frac{Q^2}{G_N M^2} < \sqrt{1 + \frac{2m_p^4}{\mu^2 M^2}} \quad (\text{A.3})$$

and

$$Q^2 < 3G_N M^2. \quad (\text{A.4})$$

The conditions in Eqs. (A.3) and (A.4) are satisfied if Eq. (2.21) holds. Similar results are obtained for individual layers.

We next notice that the condition for the existence of the quantum spectrum in Eq. (2.21) implies that

$$1 \leq \alpha \leq 2\beta_M - 1. \quad (\text{A.5})$$

We already considered the more astrophysical relevant case  $\alpha \sim 1$  for the dust ball with a relatively small amount of charge in Section 2.2. Here, we shall instead study the ground state in the opposite case when  $\alpha \sim \beta_M$ , with  $N_{MQ} \sim 1$ . From  $\beta_M = \mu M/m_p^2$ , we have

$$\alpha \sim \frac{\mu M}{m_p^2} \quad (\text{A.6})$$

and Eq. (2.7) then implies

$$Q^2 \sim G_N M^2. \quad (\text{A.7})$$

which approaches the extremal case (see Fig. 1). For the same limiting case one obtains

$$\lim_{n \rightarrow 1} \frac{\Delta R_s}{\langle n\alpha | \hat{R}_s | n\alpha \rangle} = \frac{\sqrt{4\mu^2 M^2/m_p^4 + 7 + m_p^2/\mu M}}{2(1 + 2\mu M/m_p^2)} \simeq \frac{1}{2}, \quad (\text{A.8})$$

where we used  $\beta_M \gg 1$ . We can in general conclude that the uncertainty

$$\frac{1}{3} < \frac{\Delta R_s}{\langle n\alpha | \hat{R}_s | n\alpha \rangle} < \frac{1}{2}, \quad (\text{A.9})$$

for  $\mu M/m_p^2 \gg 1$ .

## References

- [1] R. L. Arnowitt, S. Deser and C. W. Misner, Phys. Rev. **116** (1959) 1322.
- [2] R. M. Wald, “General Relativity,” (Chicago University Press, 1984)
- [3] S. W. Hawking and G. F. R. Ellis, “The Large Scale Structure of Space-Time,” (Cambridge University Press, Cambridge, 1973)
- [4] R. P. Geroch and J. H. Traschen, Phys. Rev. D **36** (1987) 1017.
- [5] H. Balasin and H. Nachbagauer, Class. Quant. Grav. **10** (1993) 2271 [arXiv:gr-qc/9305009 [gr-qc]].
- [6] J. M. McNamara, Proc. R. Soc. London **A358** (1978) 449.
- [7] Y. Gursel, V. D. Sandberg, I. D. Novikov and A. A. Starobinsky, Phys. Rev. D **19** (1979) 413.
- [8] S. Chandrasekhar and J. B. Hartle, Proc. R. Soc. London **A284** (1982) 301.
- [9] E. Poisson and W. Israel, Phys. Rev. Lett. **63** (1989) 1663.
- [10] M. L. Gnedin and N. Y. Gnedin, Class. Quant. Grav. **10** (1993) 1083.
- [11] P. R. Brady and J. D. Smith, Phys. Rev. Lett. **75** (1995) 1256 [arXiv:gr-qc/9506067 [gr-qc]].
- [12] L. M. Burko, Phys. Rev. Lett. **79** (1997) 4958 [arXiv:gr-qc/9710112 [gr-qc]].
- [13] D. Marolf and A. Ori, Phys. Rev. D **86** (2012) 124026 [arXiv:1109.5139 [gr-qc]].

- [14] E. Eilon and A. Ori, Phys. Rev. D **94** (2016) 104060 [arXiv:1610.04355 [gr-qc]].
- [15] R. Carballo-Rubio, F. Di Filippo, S. Liberati and M. Visser, [arXiv:2402.14913 [gr-qc]].
- [16] R. Balbinot and A. Fabbri, Phys. Rev. D **108** (2023) 045004 [arXiv:2303.11039 [gr-qc]].
- [17] R. Casadio and A. Giusti, Phys. Lett. B **797** (2019) 134915 [arXiv:1904.12663 [gr-qc]].
- [18] R. Casadio, Int. J. Mod. Phys. D **9** (2000) 511 [arXiv:gr-qc/9810073 [gr-qc]].
- [19] I. Kuntz and R. Casadio, Phys. Lett. B **802** (2020), 135219 [arXiv:1911.05037 [hep-th]].
- [20] I. Kuntz and R. da Rocha, Eur. Phys. J. C **79** (2019) 447 [arXiv:1903.10642 [hep-th]].
- [21] H. M. Haggard and C. Rovelli, Phys. Rev. D **92** (2015) 104020 [arXiv:1407.0989 [gr-qc]].
- [22] A. Bonanno, D. Malafarina and A. Panassiti, Phys. Rev. Lett. **132** (2024) 031401 [arXiv:2308.10890 [gr-qc]].
- [23] G. Lemaitre, Annales Soc. Sci. Bruxelles A **47** (1927) 49.
- [24] R. C. Tolman, Proc. Nat. Acad. Sci. **20** (1934) 169.
- [25] H. Bondi, Mon. Not. Roy. Astron. Soc. **107** (1947) 410.
- [26] J. R. Oppenheimer and H. Snyder, Phys. Rev. **56** (1939) 455.
- [27] A. Einstein, J. Grommer, *Allgemeine Relativitätstheorie und Bewegungsgesetz*, Sitzber. Preuss. Akad. Wiss. Berlin, **2** (1927); A. Einstein, L. Infeld, B. Hoffmann, *The Gravitational Equations and the Problem of Motion*, Ann. Math., **39**, 65 (1938).
- [28] C. Kiefer, “Quantum gravity” (Clarendon Press, 2004)
- [29] R. Casadio, Phys. Rev. D **58** (1998) 064013 [arXiv:gr-qc/9804021 [gr-qc]].
- [30] C. Vaz and L. Witten, Gen. Rel. Grav. **43** (2011) 3429 [arXiv:1111.6821 [gr-qc]].
- [31] C. Kiefer and T. Schmitz, Phys. Rev. D **99** (2019) 126010 [arXiv:1904.13220 [gr-qc]].
- [32] W. Piechocki and T. Schmitz, Phys. Rev. D **102** (2020) 046004 [arXiv:2004.02939 [gr-qc]].
- [33] T. Schmitz, Phys. Rev. D **103** (2021) 064074 [arXiv:2012.04383 [gr-qc]].
- [34] V. Husain, J. G. Kelly, R. Santacruz and E. Wilson-Ewing, Phys. Rev. D **106** (2022) 024014 [arXiv:2203.04238 [gr-qc]].
- [35] K. Giesel, M. Han, B. F. Li, H. Liu and P. Singh, Phys. Rev. D **107** (2023) 044047 [arXiv:2212.01930 [gr-qc]].
- [36] T. Jacobson, Phys. Rev. Lett. **75** (1995) 1260 [arXiv:gr-qc/9504004 [gr-qc]].
- [37] J. M. Bardeen, B. Carter and S. W. Hawking, Commun. Math. Phys. **31** (1973) 161.
- [38] J.D. Bekenstein, Phys. Rev. D **7** (1973) 2333.



- [39] R. Casadio, *Eur. Phys. J. C* **82** (2022) 10 [arXiv:2103.14582 [gr-qc]].
- [40] R. Casadio, *Phys. Lett. B* **843** (2023) 138055 [arXiv:2304.06816 [gr-qc]].
- [41] C. W. Misner and D. H. Sharp, *Phys. Rev.* **136** (1964), B571.
- [42] W. C. Hernandez and C. W. Misner, *Astrophys. J.* **143** (1966) 452.
- [43] R. Casadio, *Int. J. Mod. Phys. D* **31** (2022) 2250128 [arXiv:2103.00183 [gr-qc]].
- [44] R. Casadio, A. Giusti and J. Ovalle, *Phys. Rev. D* **105** (2022) 124026 [arXiv:2203.03252 [gr-qc]].
- [45] R. Casadio, A. Giusti and J. Ovalle, *JHEP* **05** (2023) 118 [arXiv:2303.02713 [gr-qc]].
- [46] V. N. Lukash and V. N. Stokov, *Int. J. Mod. Phys. A* **28** (2013) 1350007 [arXiv:1301.5544 [gr-qc]].
- [47] R. Carballo-Rubio, F. Di Filippo, S. Liberati and M. Visser, “Singularity-free gravitational collapse: From regular black holes to horizonless objects,” [arXiv:2302.00028 [gr-qc]].
- [48] J. Makela and P. Repo, *Phys. Rev. D* **57** (1998) 4899 [arXiv:gr-qc/9708029 [gr-qc]].
- [49] V. A. Berezin, *Phys. Rev. D* **55** (1997) 2139 [arXiv:gr-qc/9602020 [gr-qc]].
- [50] R. Casadio, *Eur. Phys. J. Plus* **139** (2024) 770 [arXiv:1305.3195 [gr-qc]].
- [51] R. Casadio and F. Scardigli, *Eur. Phys. J. C* **74** (2014) 2685 [arXiv:1306.5298 [gr-qc]].
- [52] X. Calmet and R. Casadio, *Eur. Phys. J. C* **75** (2015) 445 [arXiv:1509.02055 [hep-th]].
- [53] R. Casadio, O. Micu and D. Stojkovic, *JHEP* **05** (2015) 096 [arXiv:1503.01888 [gr-qc]].
- [54] W. Feng, A. Giusti and R. Casadio, “Horizon quantum mechanics for coherent quantum black holes,” [arXiv:2408.17091 [gr-qc]].
- [55] J. Arrechea, S. Liberati and V. Vellucci, “Whispers from the quantum core: the ringdown of semiclassical stars,” [arXiv:2407.08807 [gr-qc]].